

# Competition between Na<sup>+</sup> and Li<sup>+</sup> for Unsealed and Cytoskeleton-Depleted Human Red Blood Cell Membrane: A <sup>23</sup>Na Multiple Quantum Filtered and <sup>7</sup>Li NMR Relaxation Study

Chandra Srinivasan,\* Nicole Minadeo,\* Jason Toon,\* Daniel Graham,\*  
Duarte Mota de Freitas,\* and Carlos F. G. C. Geraldes†<sup>1</sup>

\*Department of Chemistry, Loyola University of Chicago, 6525 N. Sheridan Road, Chicago, Illinois 60626; and †Department of Biochemistry and Center for Neurosciences, University of Coimbra, P.O. Box 3126, 3000 Coimbra, Portugal

Received February 4, 1999; revised May 5, 1999

Evidence for competition between Li<sup>+</sup> and Na<sup>+</sup> for binding sites of human unsealed and cytoskeleton-depleted human red blood cell (csdRBC) membranes was obtained from the effect of added Li<sup>+</sup> upon the <sup>23</sup>Na double quantum filtered (DQF) and triple quantum filtered (TQF) NMR signals of Na<sup>+</sup>-containing red blood cell (RBC) membrane suspensions. We found that, at low ionic strength, the observed quenching effect of Li<sup>+</sup> on the <sup>23</sup>Na TQF and DQF signal intensity probed Li<sup>+</sup>/Na<sup>+</sup> competition for isotropic binding sites only. Membrane cytoskeleton depletion significantly decreased the isotropic signal intensity, strongly affecting the binding of Na<sup>+</sup> to isotropic membrane sites, but had no effect on Li<sup>+</sup>/Na<sup>+</sup> competition for those sites. Through the observed <sup>23</sup>Na DQF NMR spectra, which allow probing of both isotropic and anisotropic Na<sup>+</sup> motion, we found anisotropic membrane binding sites for Na<sup>+</sup> when the total ionic strength was higher than 40 mM. This is a consequence of ionic strength effects on the conformation of the cytoskeleton, in particular on the dimer-tetramer equilibrium of spectrin. The determinant involvement of the cytoskeleton in the anisotropy of Na<sup>+</sup> motion at the membrane surface was demonstrated by the isotropy of the DQF spectra of csdRBC membranes even at high ionic strength. Li<sup>+</sup> addition initially quenched the isotropic signal the most, indicating preferential Li<sup>+</sup>/Na<sup>+</sup> competition for the isotropic membrane sites. High ionic strength also increased the intensity of the anisotropic signal, due to its effect on the restructuring of the membrane cytoskeleton. Further Li<sup>+</sup> addition competed with Na<sup>+</sup> for those sites, quenching the anisotropic signal.

<sup>7</sup>Li T<sub>1</sub> relaxation data for Li<sup>+</sup>-containing suspensions of unsealed and csdRBC membranes, in the absence and presence of Na<sup>+</sup> at low ionic strength, showed that cytoskeleton depletion does not affect the affinity of Na<sup>+</sup> for the RBC membrane, but increases the affinity of Li<sup>+</sup> by 50%. This clearly indicates that cytoskeleton depletion favors Li<sup>+</sup> relative to Na<sup>+</sup> binding, and thus Li<sup>+</sup>/Na<sup>+</sup> competition for its isotropic sites. Thus, this relaxation technique proves to be very sensitive to alkali metal binding to the membrane, detecting a more pronounced steric hindrance effect of the

cytoskeleton network to binding of the larger hydrated Li<sup>+</sup> ion to the membrane phosphate groups. © 1999 Academic Press

**Key Words:** lithium; human red blood cell membranes; cytoskeleton; multiple-quantum-filtered <sup>23</sup>Na NMR; <sup>7</sup>Li relaxation times.

## INTRODUCTION

Lithium ion is widely used in the treatment of manic-depressive or bipolar illness, a psychiatric disorder characterized by severe mood swings (1, 2). Although lithium salts (carbonate or citrate) have been used to treat manic-depressive individuals for more than 40 years, its pharmacological mode and sites of action are still under investigation (3, 4). The two inter-related hypotheses that we are investigating at the molecular level are competition between Li<sup>+</sup> and Mg<sup>2+</sup> for Mg<sup>2+</sup>-binding sites in biomolecules, and a cell membrane abnormality. To understand the mode of action of Li<sup>+</sup>, human RBCs<sup>2</sup> were used as a model system since they were readily available and easy to handle. A detailed NMR study of the interactions of Li<sup>+</sup> within RBCs and with their components (5) revealed that the inner leaflet of the plasma membrane provides a major binding site for Li<sup>+</sup>, while SA does not contribute significantly toward Li<sup>+</sup> binding, as opposed to what had been previously postulated (6).

<sup>23</sup>Na MQF spectroscopy is a powerful tool for the detailed study of the membrane molecular sites of Na<sup>+</sup> and Li<sup>+</sup> binding, and, in particular, for investigation of the involvement of the cytoskeleton network. It is well known that quadrupolar nuclei with spin  $I = \frac{3}{2}$ , such as <sup>23</sup>Na, <sup>39</sup>K, and <sup>87</sup>Rb, may exhibit biexponential spin relaxation in systems where they rapidly

<sup>2</sup> Abbreviations: DQF, double quantum filtered; Hepes, [4-(2-hydroxyethyl)-1-piperazineethanesulfonic acid]; I, nuclear spin; MQF, multiple quantum filtered; NMR, nuclear magnetic resonance; PW, pulse width; RBCs, red blood cells; csdRBC membranes, cytoskeleton-depleted human RBC membranes; SA, spectrin-actin; SDS-PAGE, sodium dodecyl sulfate-polyacrylamide gel electrophoresis; SQ, single quantum; T<sub>1</sub>, spin-lattice relaxation time; T<sub>2</sub>, spin-spin relaxation time; TQF, triple quantum filtered; τ<sub>c</sub>, correlation time; ω, radiofrequency; ω<sub>Q</sub>, residual quadrupole splitting.

<sup>1</sup> To whom correspondence should be addressed at Department of Biochemistry, Faculty of Science and Technology and Center for Neurosciences, University of Coimbra, P.O. Box 3126, 3000 Coimbra, Portugal. E-mail: geraldes@cygnus.ci.uc.pt.

exchange between free and nonextreme narrowing motional bound states. The biexponential transverse (spin-spin) relaxation can be described by a faster decay rate of the outer transitions ( $-\frac{3}{2} \leftrightarrow -\frac{1}{2}$  and  $\frac{1}{2} \leftrightarrow \frac{3}{2}$ ) relative to the inner transition ( $-\frac{1}{2} \leftrightarrow \frac{1}{2}$ ), but such a description does not apply to biexponential longitudinal (spin-lattice) relaxation (7, 8). This biexponential relaxation behavior allows the creation and detection of multiple quantum coherences (9, 10). MQF NMR spectroscopy of quadrupolar  $I = \frac{3}{2}$  alkali metal nuclei has been studied extensively in macromolecular model systems (11–15) and in perfused organs, such as rat salivary glands (16), rat and guinea-pig hearts (17–22), and rat liver (23). It was also applied to *in vivo* organs, such as rat liver (24), human brain, and skeletal muscle (25). In particular, <sup>23</sup>Na MQF NMR experiments have proven to be powerful tools for measuring biexponential relaxation rates of sodium ions in biological systems (26, 27) and in the measurement of intracellular sodium concentration (28).

In isotropic systems, DQF and TQF spectra are identical except for a 50% increased efficiency of the TQF coherence formation (29). This results from the fact that in the isotropic phase, as the outer transitions are degenerate, biexponential relaxation only creates the third-rank tensor  $T_{31}$ , which evolves into both DQ and TQ coherence tensors  $T_{32}$  and  $T_{33}$ , respectively (10). The DQF and TQF signals for isotropic systems thus consist of a positive  $T_{31}$  signal with a lineshape resulting from two Lorentzian lines in antiphase. In ordered systems, with a static quadrupolar interaction, or in partially ordered systems, where the average quadrupolar interaction  $\bar{\omega}_Q$  is non-zero, the degeneracy of the outer spin transitions is lifted and the even-rank tensor  $T_{21}$  can be formed (10). This results in the detection in the DQF spectra of a broad negative component presenting a pair of overlapping dispersive lines of the satellites in antiphase, split by  $2\bar{\omega}_Q$  (12). Anisotropic motion of Na<sup>+</sup> ions has been detected using this method (30) in a variety of biological systems, such as RBCs (12, 14), connective tissues—cartilage, tendon and skin (13, 31–33), perfused rat hearts (22, 34), rat brain (35), and *in vivo* human skeletal muscle and brain (25), as well as cartilage (36). In RBCs the anisotropic sodium binding sites are present at the membrane level in both the intra- and extracellular compartments and depend on the integrity of the cytoskeleton (12, 14, 37, 38).

Although <sup>7</sup>Li MQF NMR experiments would provide a direct approach to address the question of Li<sup>+</sup> binding, the weak quadrupolar moment of the <sup>7</sup>Li nucleus, with very long spin-lattice relaxation times (usually in seconds), has thus far made these measurements unsuccessful (39). Hence the indirect approach of monitoring the effect of Li<sup>+</sup> addition on the <sup>23</sup>Na MQF NMR signal was primarily used in this study. The <sup>23</sup>Na DQF NMR signals of sodium ions in both the intra- and extracellular compartments of human RBCs are quenched in the presence of increasing concentrations of Li<sup>+</sup> in each compartment (37). Here we present evidence for competition between Li<sup>+</sup> and Na<sup>+</sup> for unsealed and csdRBC membranes using

the effect of Li<sup>+</sup> addition upon the <sup>23</sup>Na DQF and TQF NMR signals. We also conducted complementary <sup>7</sup>Li  $T_1$  relaxation measurements to study Li<sup>+</sup>/Na<sup>+</sup> competition for the two types of preparation of human RBC membrane. Thus, a much more complete picture of the molecular sites of Li<sup>+</sup>/Na<sup>+</sup> competition for the RBC membrane and of the role played by the cytoskeleton on that process is obtained in this work.

## EXPERIMENTAL

**Materials.** Fresh human RBCs were obtained from a blood bank (Life Source, Chicago, IL) and they were processed within 2–3 days. Inorganic chemicals such as NaCl, LiCl, MgCl<sub>2</sub>, and EDTA were of high purity and were purchased from Sigma Chemical Company. Hepes in free acid form was used to prepare Hepes buffer, which was also from Sigma.

**Preparation of unsealed and cytoskeleton depleted RBC membranes.** The procedure for the preparation of unsealed RBC membranes was adapted from the literature (40) and the modified procedure was published in our previous articles (5, 41). Briefly, washed RBCs were lysed using 5 mM Hepes buffer at pH 8.0 and the suspension was centrifuged at 22,000 g at 4°C for 15 min; the supernatant was discarded while the pellet was washed until pale pink membranes were obtained. Removal of the cytoskeleton was accomplished according to a published procedure (42). Incubation of 2 mL of the unsealed RBC membranes in 18 mL of 0.1 mM EDTA at pH 8.0 and at 37°C for 30 min, was followed by centrifugation of the suspension at 22,000 g and 4°C to remove the supernatant containing the cytoskeleton. The pellet was washed twice with 5 mM Hepes buffer at pH 8.0 to ensure complete removal of the cytoskeleton and to prevent EDTA contamination of the sample. The removal of cytoskeleton was monitored by the decrease in protein concentration (43) in the membrane pellet relative to the unsealed RBC membrane, and the presence of SA in the supernatant by SDS-PAGE (44). The pellet was finally made up to a volume of 2.0 mL using 5 mM Hepes buffer at pH 8.0 and required amounts of NaCl or LiCl were added using a highly concentrated stock solution so that the volume change was minimal.

**NMR experiments.** <sup>23</sup>Na SQ NMR experiments were conducted using a Varian Unity 500 NMR spectrometer, operating at 132.212 MHz, using a broadband 10 mm probe tuned for sodium, and 10 mm o.d. sample tubes. Typically a spectral width of 2500 Hz in 4K complex points was acquired. Other typical conditions were: line broadening for signal-to-noise enhancement, 10 Hz; 90° RF pulse width, 23 μs; pulse delay, 100 ms; acquisition time, 410 ms.

<sup>23</sup>Na MQF NMR spectra were measured at 132.212 MHz using a Varian Unity 500 NMR spectrometer. The DQF and TQF  $T_2$  measurements were performed using the pulse sequence

$$90^\circ - \tau / 2 - 180^\circ - \tau / 2 - \theta^\circ - \delta - \theta^\circ - t_{\text{acq}} \quad [1]$$

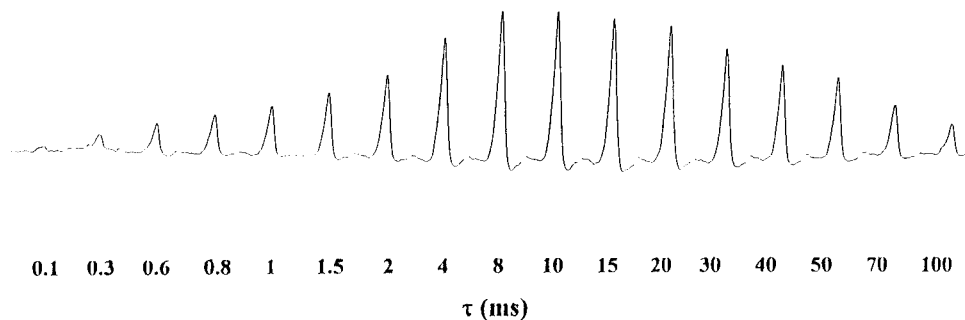


**FIG. 1.**  $^{23}\text{Na}$  TQF spectra as a function preparation time of unsealed RBC membranes in the presence of 5 mM NaCl at 25°C.

with  $\theta = 90^\circ$  and  $54.7^\circ$  for DQF and  $\theta = 90^\circ$  for TQF. In this sequence  $\tau$  is the creation or preparation time,  $\delta$  is the evolution time, and  $t_{\text{acq}}$  is the acquisition time (9, 10). The evolution time was fixed at 10  $\mu\text{s}$ , while the preparation time varied. This was changed typically in 20 steps, from 0.1 to 300 ms. Although we used the same pulse sequence for both DQF and TQF experiments, each type of spectrum was selected through suitable phase cycling (128 steps for DQF, 384 for TQF) (45). Special care was taken to calibrate the  $90^\circ$  pulse width accurately for each sample and the carrier frequency was selected to coincide with the SQ signal. The performance of the DQ and TQ filter was checked for any SQ signal leakage by running a 150 mM NaCl sample in  $\text{D}_2\text{O}$ , and observing the absence of DQF and TQF signals from monoexponential free  $\text{Na}_{\text{aq}}^+$  ions. The performance of the DQ and TQ filter in the RBC membrane preparations was checked using a sample of RBC membrane containing 5 mM NaCl and 10 mM LiCl. This was done through observation of the effects of any missettings of the  $90^\circ$  pulse width on the lineshape and intensity of the DQF and TQF signal. A change of up to  $\pm 1 \mu\text{s}$  from the measured  $90^\circ$  pulse width did not affect the shape or the intensity of the MQF signal significantly. All NMR spectra were recorded at 37°C and the MQF spectra were recorded without spinning. All NMR measurements were repeated twice using two separately prepared samples to confirm the reproducibility of the results.

$^7\text{Li}$  NMR measurements were conducted at 116.5 MHz on a Varian VXR-300 NMR spectrometer, equipped with a multinuclear probe at 37°C, using nonspinning 10 mm NMR tubes.  $T_1$  measurements of  $^7\text{Li}$  NMR resonances were done by the inversion recovery method.

**Data processing.** Post-processing of all FIDs included baseline correction before Fourier transformation. SQ  $T_1$  values were determined using the nonlinear least-square three parameter fit procedure of the Varian software. For DQF and TQF spectra, a magnitude calculation was done after Fourier transformation. The areas under the resultant peaks were determined by point-to-point integration between user-defined break points. The values of  $T_{2f}$ ,  $T_{2s}$ , and  $\bar{\omega}_Q$  were obtained by fitting the DQF or TQF signal peak area versus the  $\tau$  value data to the appropriate function (see later) using a Marquart–Levenberg nonlinear optimization algorithm. The goodness of

the nonlinear regressions was evaluated by the minimization of the corresponding  $\chi^2$  (sums of the square deviations) values.

The  $\text{Li}^+$  binding constant,  $K_b$ , to the RBC membrane was calculated from a James–Noggle plot (46),

$$\begin{aligned} \Delta R^{-1} &= (R_{\text{obs}} - R_f)^{-1} \\ &= K_{\text{Li}}^{-1} \{ [\text{B}] (R_b - R_f) \}^{-1} + [\text{Li}^+]_t \{ [\text{B}] (R_b - R_f) \}^{-1}, \end{aligned} \quad [2]$$

where  $R_{\text{obs}}$ ,  $R_f$ , and  $R_b$  are the reciprocals of the observed ( $T_{1\text{obs}}$ ), free ( $T_{1f}$ ) and bound ( $T_{1b}$ ) spin–lattice relaxation values,  $[\text{Li}^+]_t$  is the total  $\text{Li}^+$  concentration, and  $[\text{B}]$  is the concentration of binding sites. This equation, which assumes 1:1 stoichiometry for the binding of  $\text{Li}^+$  to binding sites in the membrane, is valid when  $[\text{Li}^+]_t \gg [\text{B}]$  (5).

## RESULTS

$^{23}\text{Na}$  TQF and DQF spectra for unsealed or csdRBC membranes suspended in media containing either 5 or 50 mM NaCl were obtained as a function of creation time, as Fig. 1 illustrates. The TQF signals exhibit the typical MQF lineshape of the  $T_{31}$  signal, with antiphase components expected for the difference of two exponentials (Fig. 1), characteristic of isotropic tumbling of  $\text{Na}^+$  ions (12). The signal intensity is modulated by the preparation time, as shown in Fig. 2. The experimental points were fitted to a double exponential of the form

$$S(\omega, \tau) = A[\exp(-\tau/T_{2s}) - \exp(-\tau/T_{2f})], \quad [3]$$

where  $\tau$  is the preparation time,  $T_{2f}$  and  $T_{2s}$  are the fast and slow components, respectively, of the biexponential spin–spin relaxation time ( $T_2$ ) (9, 32).

The effect of  $\text{Li}^+$  on the TQF signals of unsealed or csdRBC membranes containing 5 or 50 mM NaCl in the suspension medium was studied in order to evaluate the extent of  $\text{Na}^+/\text{Li}^+$  competition toward membrane binding sites and to understand the contribution of the cytoskeleton to ion binding. In all cases, a quenching effect of  $\text{Li}^+$  on the  $^{23}\text{Na}$  TQF signal intensity of

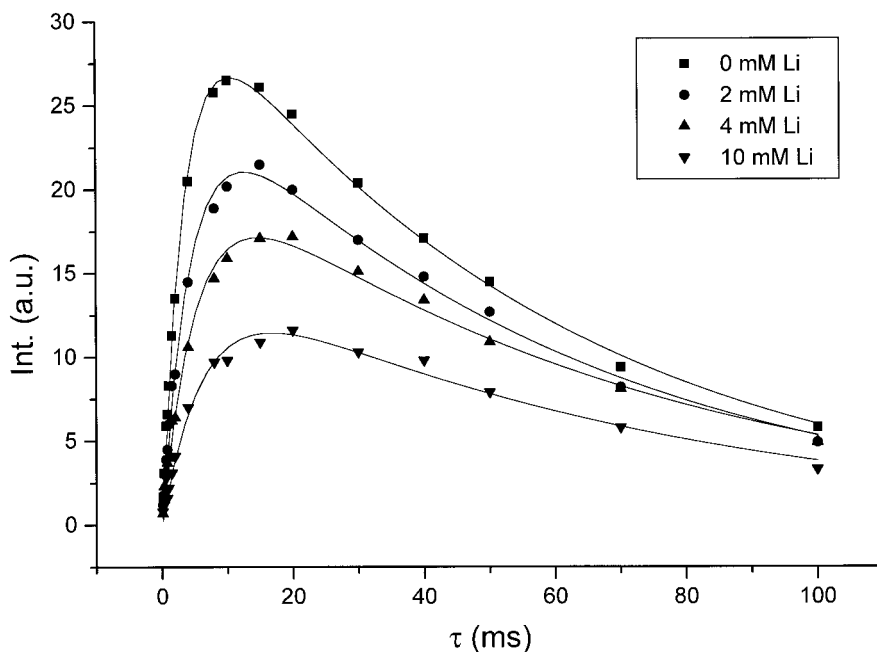


**FIG. 2.** <sup>23</sup>Na TQF NMR signal intensity versus preparation time at increasing LiCl concentrations of unsealed RBC membranes in the presence of 5 mM NaCl at 25°C. The solid lines correspond to calculated curves using the parameters in Table 1, resulting from nonlinear least-squares fitting of the data.

Na<sup>+</sup> containing membrane solutions was observed, in agreement with the reported quenching effect of the lithium ion on the <sup>23</sup>Na DQF signals of both the intracellular and the extracellular compartments in human RBCs (37). Figure 2 compares the dependence of the TQF signal intensity on preparation time for a membrane sample containing 5 mM NaCl before and after addition of increasing amounts of LiCl. The experimental data were fitted well by Eq. [3], except for the unsealed RBC membranes when the total ionic strength was higher than 40 mM (all the membrane samples with 50 mM NaCl and increasing LiCl, and the membrane sample with 5 mM NaCl and 40 mM LiCl). Equation [3] applies to isotropic samples with zero residual quadrupole splittings,  $\bar{\omega}_Q = 0$ , a condition which is not found in the latter samples, as shown by their <sup>23</sup>Na DQF signals (see below). Table 1 lists the various parameters obtained by fitting the experimental curves, for the various Li<sup>+</sup>/Na<sup>+</sup> concentration ratios, in the isotropic samples. The calculated parameters include  $A$ ,  $T_{2f}$ , and  $T_{2s}$ , as well as the values of the preparation time  $\tau_{\max}$  which give the  $I_{\max}$  values, the maximum TQF signal intensities. The  $I_{\max}$  values are naturally higher for samples containing 50 mM NaCl than for 5 mM NaCl, because they increase with the single quantum magnetization  $M_o$ , which in turn increases with the Na<sup>+</sup> concentration. However, at a given Na<sup>+</sup> concentration  $I_{\max}$  is larger for intact RBC membranes than for csdRBC membranes. This significant decrease of the  $T_{31}$  TQF signal intensity upon cytoskeleton depletion of the membranes shows that binding of Na<sup>+</sup> to isotropic membrane sites is strongly affected by the presence of the cytoskeleton network and by its conformational changes induced by an increase in ionic strength (12). Table 1 also

shows the dependence of  $\tau_{\max}$  on Na<sup>+</sup> concentration and the presence of the cytoskeleton, with a significant decrease when Na<sup>+</sup> decreases from 50 to 5 mM. This is a reflection of the large decrease of the  $T_{2f}$  and  $T_{2s}$  values at lower Na<sup>+</sup> concentrations. Such a decrease of  $T_{2f}$  to very short values reflects a larger percentage of Na<sup>+</sup> ions bound to the membrane at lower concentrations.

The extent of quenching of the <sup>23</sup>Na TQF  $T_{31}$  signal intensity by Li<sup>+</sup> at increasing Li<sup>+</sup>/Na<sup>+</sup> ratios was examined. Figure 3A shows plots of the dependence of the intensity ( $A$ ) of the  $T_{31}$  signal on the ratio ( $\rho$ ) of LiCl to NaCl concentrations for the isotropic unsealed and csdRBC membranes. This allows the quantitative evaluation of the parameter  $\Delta A(\%)$  (see Table 1), which gives the percentage decrease of the TQF peak intensity due to the replacement of Na<sup>+</sup> ions, bound at the membrane isotropic sites, by Li<sup>+</sup> ions. At 5 mM NaCl, the percentage of quenching is the same in intact and csdRBC membranes, at all Li<sup>+</sup>/Na<sup>+</sup> ratios, indicating that, at this low ionic strength, removal of the cytoskeleton has no effect on Li<sup>+</sup>/Na<sup>+</sup> competition for the membrane isotropic sites. This is not surprising because the cytoskeleton is expected to be at least partially released from the membrane at low ionic strength (42); unsealed membrane suspensions containing 5 mM NaCl will therefore contain free cytoskeleton and will have isotropic sites exposed just like csdRBC membrane suspensions containing 5 mM NaCl. However, for the csdRBC membranes at 50 mM NaCl, that percentage of quenching is much higher than for the other cases.

The effect of Li<sup>+</sup> addition on the value of  $\tau_{\max}$  for the TQF signal, also shown on Table 1, is highly dependent on the

TABLE 1

<sup>23</sup>Na TQF and DQF NMR Parameters, Obtained from Curve Fitting,<sup>a</sup> for Unsealed and csd-RBC Membranes, in the Presence of Varying Concentrations of NaCl and LiCl (Cases where No  $T_{21}$  Signal is Present for DQF, Isotropic Samples,  $\bar{\omega}_Q = 0$ )

Sample	MQF	[Li <sup>+</sup> ] (mM)	A (a.u.)	$T_{2f}$ (ms)	$T_{2s}$ (ms)	$I_{\max}$ (a.u.)	$\tau_{\max}$ (ms)	$\bar{\omega}_Q$ (Hz)	$\Delta A$ (%) <sup>b</sup>	$\chi^2$
RBC memb. 5 mM NaCl	TQF	0.0	34 ( $\pm 1$ )	3.5 ( $\pm 0.1$ )	57.6 ( $\pm 1.0$ )	26.5	11	—	0	0.22
		2.0	28 ( $\pm 1$ )	4.5 ( $\pm 0.1$ )	60.2 ( $\pm 1.6$ )	21.5	15	—	18	0.35
		4.0	23 ( $\pm 1$ )	5.3 ( $\pm 0.2$ )	66.5 ( $\pm 2.4$ )	17.2	20	—	32	0.40
		10.0	16 ( $\pm 1$ )	6.3 ( $\pm 0.2$ )	69.8 ( $\pm 3.2$ )	11.6	21	—	53	0.33
	DQF	0.0	39 ( $\pm 1$ )	2.7 ( $\pm 0.1$ )	58.1 ( $\pm 1.9$ )	32.0	9	—	0	1.14
		2.0	29 ( $\pm 1$ )	5.0 ( $\pm 0.1$ )	62.5 ( $\pm 1.2$ )	21.6	12	—	26	0.18
		4.0	26 ( $\pm 1$ )	6.5 ( $\pm 0.3$ )	61.9 ( $\pm 2.5$ )	16.8	15	—	33	0.65
		10.0	16 ( $\pm 1$ )	7.1 ( $\pm 0.4$ )	58.5 ( $\pm 3.7$ )	11.4	17	—	59	0.39
CsdRBC memb. 50 mM NaCl	TQF	0.0	58 ( $\pm 2$ )	10.2 ( $\pm 0.6$ )	83.7 ( $\pm 4.6$ )	37.4	30	—	0	6.65
		10.0	39 ( $\pm 2$ )	8.9 ( $\pm 0.6$ )	92.1 ( $\pm 5.6$ )	27.0	30	—	33	3.95
		20.0	28 ( $\pm 2$ )	6.9 ( $\pm 0.6$ )	99.5 ( $\pm 7.7$ )	20.7	30	—	52	3.48
		40.0	21 ( $\pm 2$ )	5.7 ( $\pm 0.7$ )	88.2 ( $\pm 8.8$ )	14.4	30	—	64	3.19
		60.0	14 ( $\pm 1$ )	3.8 ( $\pm 0.4$ )	102.3 ( $\pm 9.2$ )	10.6	25	—	76	1.21
		10.0	27 ( $\pm 1$ )	11.2 ( $\pm 0.5$ )	86.2 ( $\pm 3.6$ )	17.4	30	—	47	0.75
	DQF	0.0	70 ( $\pm 1$ )	11.6 ( $\pm 0.5$ )	84.3 ( $\pm 3.6$ )	43.8	27	—	0	5.23
		10.0	27 ( $\pm 1$ )	11.2 ( $\pm 0.5$ )	86.2 ( $\pm 3.6$ )	17.4	30	—	47	0.75
		20.0	19 ( $\pm 1$ )	12.0 ( $\pm 0.5$ )	102.4 ( $\pm 4.7$ )	12.3	40	—	73	0.44
		40.0	13 ( $\pm 1$ )	9.7 ( $\pm 0.6$ )	85.1 ( $\pm 4.4$ )	8.4	30	—	81	0.29
		60.0	11 ( $\pm 1$ )	8.9 ( $\pm 0.4$ )	68.0 ( $\pm 2.5$ )	6.8	20	—	84	0.10
		10.0	19 ( $\pm 1$ )	12.0 ( $\pm 0.5$ )	102.4 ( $\pm 4.7$ )	12.3	40	—	73	0.44
CsdRBC memb. 5 mM NaCl	TQF	0.0	23 ( $\pm 1$ )	2.8 ( $\pm 0.1$ )	52.7 ( $\pm 1.6$ )	18.9	10	—	0	0.38
		2.0	19 ( $\pm 1$ )	4.4 ( $\pm 0.2$ )	59.5 ( $\pm 1.9$ )	14.3	15	—	17	0.26
		4.0	15 ( $\pm 1$ )	3.8 ( $\pm 0.3$ )	61.6 ( $\pm 3.3$ )	11.0	17	—	35	0.45
		10.0	11 ( $\pm 1$ )	6.0 ( $\pm 0.4$ )	66.0 ( $\pm 3.8$ )	7.3	20	—	52	0.28
		40.0	8 ( $\pm 2$ )	14.1 ( $\pm 0.7$ )	40.2 ( $\pm 1.8$ )	3.0	22	—	65	0.04
		10.0	11 ( $\pm 1$ )	6.0 ( $\pm 0.4$ )	66.0 ( $\pm 3.8$ )	7.3	20	—	52	0.28
	DQF	0.0	15 ( $\pm 1$ )	2.8 ( $\pm 0.1$ )	55.8 ( $\pm 1.3$ )	12.2	10	—	0	0.10
		2.0	14 ( $\pm 1$ )	6.4 ( $\pm 0.3$ )	63.6 ( $\pm 2.4$ )	9.6	15	—	7	0.18
		4.0	9 ( $\pm 1$ )	4.0 ( $\pm 0.3$ )	76.6 ( $\pm 5.3$ )	7.2	18	—	40	0.28
		10.0	8 ( $\pm 1$ )	7.5 ( $\pm 0.4$ )	71.0 ( $\pm 3.1$ )	6.0	20	—	47	0.10
		40.0	7 ( $\pm 1$ )	21.0 ( $\pm 1$ )	43.8 ( $\pm 1.2$ )	1.8	35	—	50	0.01
		10.0	19 ( $\pm 1$ )	12.0 ( $\pm 0.5$ )	102.4 ( $\pm 4.7$ )	12.3	40	—	73	0.44

<sup>a</sup> Using Eq. 3,  $\bar{\omega}_Q = 0$ .

<sup>b</sup> Decrease of the TQF or DQF peak intensity, given by A value, in the presence of LiCl, relative to the intensity before LiCl addition.

solution ionic strength. At 5 mM NaCl concentration in the suspension medium, both types of membranes show a marked increase of  $\tau_{\max}$  upon Li<sup>+</sup> addition, which results from increased  $T_{2f}$  and  $T_{2s}$  values. At this low NaCl concentration, the observed increase of the relaxation time components, especially of  $T_{2f}$ , upon LiCl addition up to a total ionic strength of 15 mM, corresponds to that expected from replacement of Na<sup>+</sup> by Li<sup>+</sup> at membrane binding sites. However, the csdRBC membranes at 50 mM NaCl show constant  $\tau_{\max}$  values upon Li<sup>+</sup> addition up to a total ionic strength of 110 mM, resulting from a decrease of  $T_{2f}$  while  $T_{2s}$  increases slightly.

The DQF signal evolution as a function of preparation time was also studied for suspensions of unsealed and csdRBC membranes containing 5 and 50 mM NaCl. For intact RBC membranes in the presence of 5 mM NaCl, as well as for csdRBC membranes at 5 and 50 mM NaCl, only the  $T_{31}$  component, characteristic of isotropic motion, was observed. The effect of Li<sup>+</sup> on the preparation time dependence of the DQF signals from these isotropic samples was also analyzed. The samples containing csdRBC membranes showed a marked

quenching of the isotropic  $T_{31}$  signal upon Li<sup>+</sup> addition, a behavior similar to what has been found for the TQF signal. For the intact unsealed membranes at 5 mM NaCl, Li<sup>+</sup> quenches the isotropic  $T_{31}$  signal, which is again the only signal present in the absence of Li<sup>+</sup> and in its presence up to 40 mM. Li<sup>+</sup> has previously been shown to quench the <sup>23</sup>Na DQF signals of both the intracellular and the extracellular compartments in human RBCs (35). As the intensity of the isotropic  $T_{31}$  component of the DQF signal has, for isotropic samples, the same preparation time modulation as the TQF signal (32), it is also described by Eq. [3]. Table 1 shows the various parameters obtained by fitting the experimental curves to Eq. [3] for the various membrane samples and Li<sup>+</sup>/Na<sup>+</sup> ratios. It can be seen that all parameters obtained from the analysis of the TQF and DQF  $T_{31}$  signal (Table 1) agree very well.

However, we found anisotropic behavior of <sup>23</sup>Na DQF signals for the unsealed RBC membranes when the total ionic strength was higher than 40 mM (all the membrane samples with 50 mM NaCl and increasing LiCl, and the membrane sample with 5 mM NaCl and 40 mM LiCl). The DQF spectra

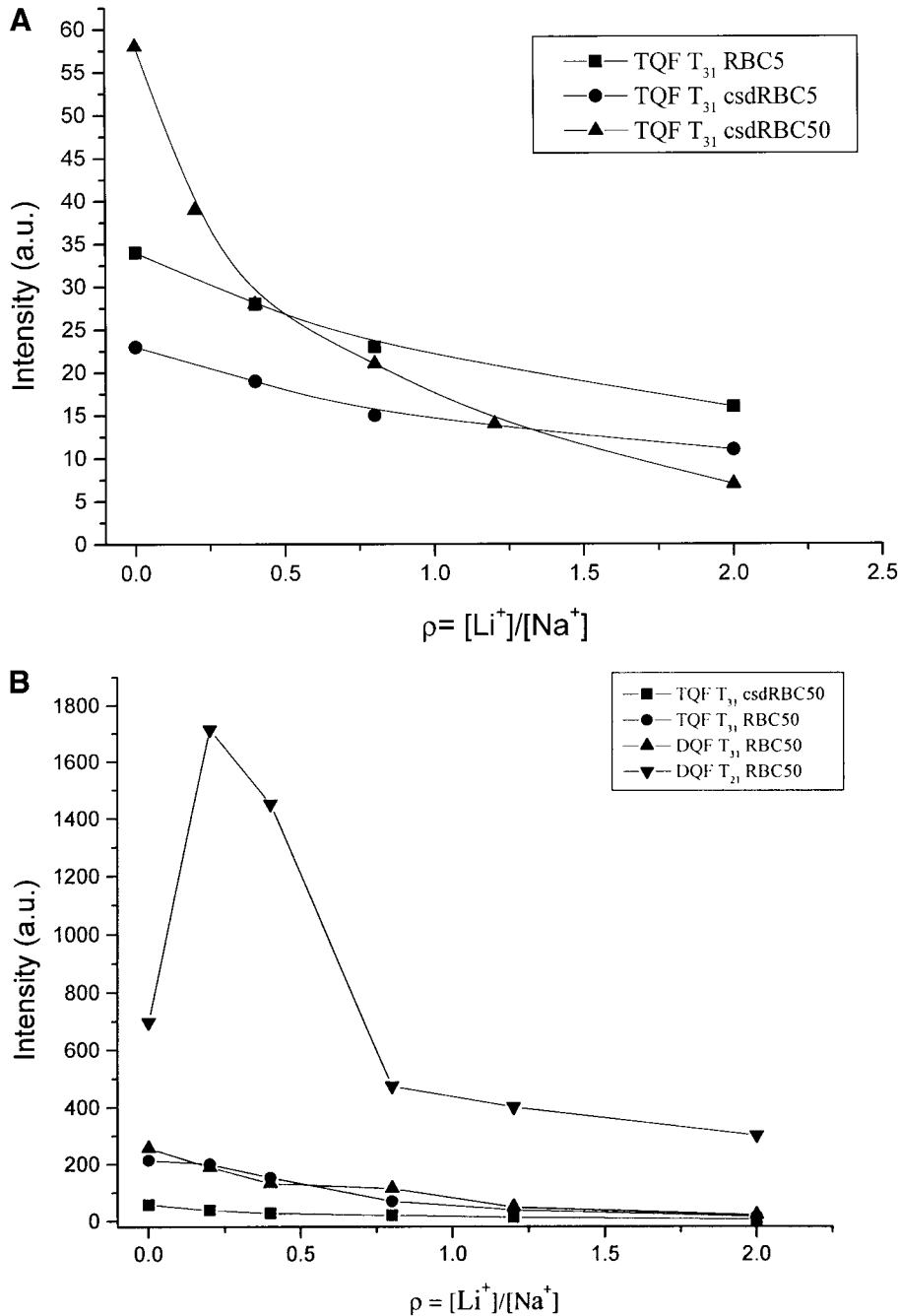


**FIG. 3.** Intensity of the  $T_{31}$  and  $T_{21}$  components of the  $^{23}\text{Na}$  TQF and DQF NMR signal vs the ratio  $\rho$  of LiCl to NaCl concentrations for the isotropic unsealed and csdRBC membranes in the presence of 5 and 50 mM NaCl: (A) TQF  $T_{31}$  for the isotropic spectra; (B) TQF and DQF  $T_{31}$  and  $T_{21}$  for the anisotropic spectra.

with  $\theta = 90^\circ$  for the intact membranes at 50 mM NaCl already show a superposition of two components, whose proportions depend on the preparation time (see Fig. 4A). The broader negative  $T_{21}$  signal, characteristic of anisotropic motion of the  $\text{Na}^+$  ions at the membrane surface, is dominant at short preparation times, but disappears at values longer than 40 ms. The narrower positive component  $T_{31}$ , arising from both isotropic

and anisotropic motion, continues to evolve at longer preparation times. This has been observed previously for unsealed RBC membranes and ghosts (12, 14, 37, 38) and is attributed to ionic strength effects on the conformation of the cytoskeleton (12), in particular on the dimer-tetramer equilibrium of spectrin (14). The cytoskeleton is involved in the anisotropy of  $\text{Na}^+$  motion at the membrane, as shown by the observed

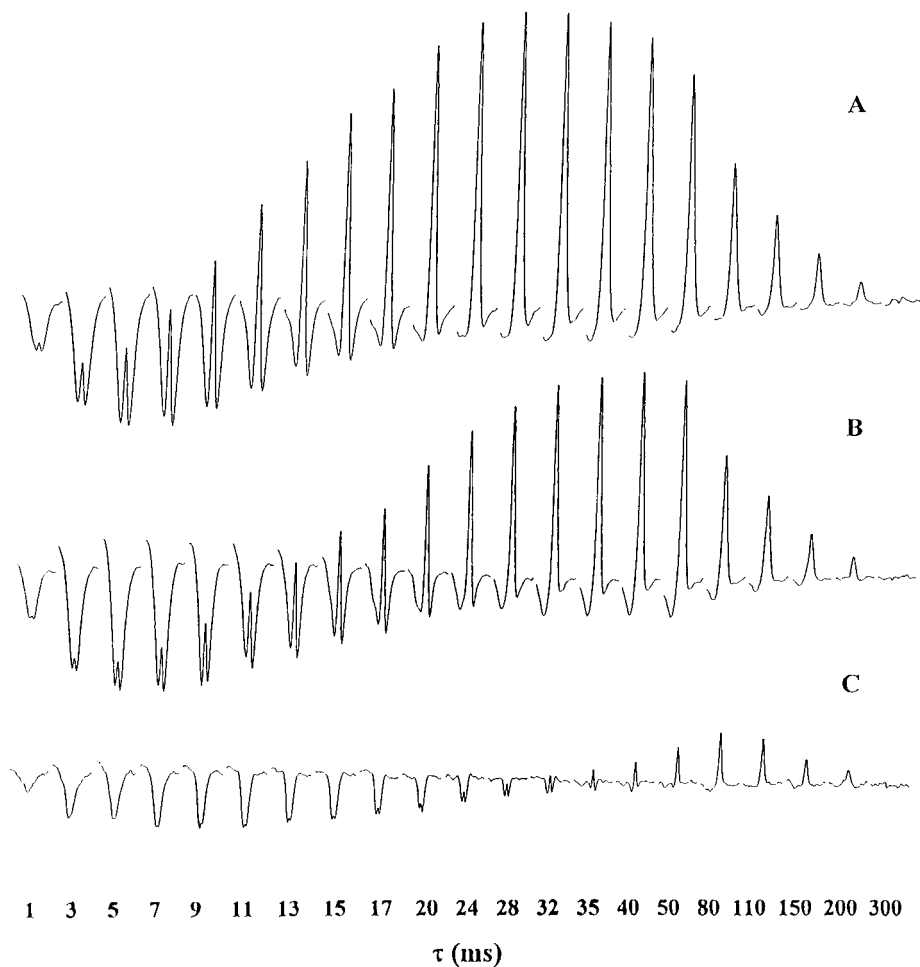


**FIG. 4.**  $^{23}\text{Na}$  DQF ( $\theta = 0^\circ$ ) NMR spectra vs preparation time for unsealed RBC membranes in the presence of 50 mM NaCl in the absence (A) and in the presence of 10 mM LiCl (B) and 40 mM LiCl (C).

isotropic DQF spectra ( $T_{31}$  component only) of csdRBC membranes in the presence of 50 mM NaCl (see Table 1) (12). When  $\text{Li}^+$  is added to this sample up to a  $\text{Li}^+/\text{Na}^+$  ratio of 2.0, both the anisotropic  $T_{21}$  signal and the  $T_{31}$  signal are quenched, as shown by Figs. 4B and C.

Addition of 40 mM LiCl to the sample of unsealed RBC membranes with 5 mM NaCl also quenched the  $T_{31}$  signal of the DQF significantly and led to the appearance of an anisotropic  $T_{21}$  signal at low preparation times. This signal evolves and disappears for preparation times higher than 30 ms. Such an anisotropy results from ionic strength effects on the membrane cytoskeleton, besides the ion competition for the membrane sites, that quenches the isotropic signal.

The  $T_{21}$  component of the DQF signal was observed separately from the  $T_{31}$  component by using the DQF pulse sequence with  $\theta = 54.7^\circ$  for all the anisotropic samples (12, 14). Deconvolution of the DQF signals with  $\theta = 90^\circ$  gave the intensities of both components as a function of preparation time. The quenching effect of  $\text{Li}^+$  addition on the intensities of the TQF ( $T_{31}$  component only) and DQF (both  $T_{31}$  and  $T_{21}$

components) signals in the anisotropic samples was then analyzed. In these cases, where the residual quadrupolar coupling constant is nonzero,  $\bar{\omega}_Q \neq 0$ , the modulation of the  $T_{31}$  component intensity of the TQF signal by the  $\tau$  value is given by (32)

$$S(\omega, \tau) = A[\exp(-\tau/T_{2s}) - \exp(-\tau/T_{2f})\cos(\bar{\omega}_Q\tau)]. \quad [4]$$

For a disordered, chemically heterogeneous system, with a series of nonequivalent binding compartments in slow exchange, with different local quadrupolar coupling constants  $\bar{\omega}_Q^{\text{loc}}$  and local directors at angles  $\theta$  with the magnetic field, each compartment has a  $\bar{\omega}_Q$  value given by  $\bar{\omega}_Q = (\bar{\omega}_Q^{\text{loc}}/2)(3\cos^2\theta - 1)$ . The TQF signal is the sum over all those contributions, with weights of the orientational distributions depending on  $\bar{\omega}_Q^{\text{loc}}$  (12, 14, 32), with a change of lineshape with  $\tau$ . Fitting of all spectral lineshapes, and assuming an orientational distribution model leads to full characterization of such systems (32). In this work, we used the simplifying assumption that the system

TABLE 2

<sup>23</sup>Na TQF and DQF NMR Parameters, Obtained from Curve Fitting, for RBC Membranes, in the Presence of 50 mM NaCl and Increasing Concentrations of LiCl (Cases where a  $T_{21}$  Signal is Present for DQF, Anisotropic Samples,  $\bar{\omega}_Q \neq 0$ )

MQF	[Li <sup>+</sup> ] (mM)	A (a.u.)	$\Delta A$ (%) <sup>a</sup>	$T_{2r}$ (ms)	$T_{2d}$ (ms)	$I_{\max}$ (a.u.)	$\tau_{\max}$ (ms)	$\bar{\omega}_Q$ (Hz)	B (a.u.)	$\Delta B$ (%) <sup>b</sup>	$\chi^2$
TQF	0.0	215 ( $\pm 1$ )	0	8.4 ( $\pm 0.1$ )	55.0 ( $\pm 1.3$ )	132	20	—	—	—	3.53
T31 (Eq. [3])	10.0	200 ( $\pm 1$ )	7	9.3 ( $\pm 0.1$ )	56.9 ( $\pm 0.4$ )	117	21	—	—	—	1.15
	20.0	153 ( $\pm 1$ )	29	10.0 ( $\pm 0.1$ )	60.3 ( $\pm 0.5$ )	88	24	—	—	—	1.27
	40.0	70 ( $\pm 1$ )	67	7.3 ( $\pm 0.2$ )	80.3 ( $\pm 1.7$ )	49	24	—	—	—	1.78
	100.0	17 ( $\pm 2$ )	92	6.3 ( $\pm 0.3$ )	79.9 ( $\pm 3.4$ )	12.5	24	—	—	—	0.46
TQF	0.0	191 ( $\pm 3$ )	0	8.4 ( $\pm 0.2$ )	60.7 ( $\pm 1.5$ )	120	19	10.0 ( $\pm 1$ )	—	—	0.74
T31 (Eq. [4])	10.0	190 ( $\pm 2$ )	0.5	9.3 ( $\pm 0.2$ )	58.6 ( $\pm 1.5$ )	113	20	6.2 ( $\pm 1$ )	—	—	0.82
	20.0	152 ( $\pm 2$ )	20	10.0 ( $\pm 0.2$ )	60.6 ( $\pm 1.5$ )	89	22	4.2 ( $\pm 1$ )	—	—	1.41
	40.0	71 ( $\pm 1$ )	63	7.4 ( $\pm 0.1$ )	78.9 ( $\pm 2.0$ )	50	19	3.5 ( $\pm 1$ )	—	—	1.96
	100.0	17 ( $\pm 1$ )	91	6.2 ( $\pm 0.1$ )	80.9 ( $\pm 2.0$ )	12.6	17	2.0 ( $\pm 1$ )	—	—	0.51
DQF	0.0	256 ( $\pm 3$ )	0	7.5 ( $\pm 0.4$ )	76.2 ( $\pm 1.9$ )	202	20	11.1 ( $\pm 0.3$ )	—	—	12.50
T31	10.0	190 ( $\pm 2$ )	26	8.0 ( $\pm 0.7$ )	82.6 ( $\pm 2.0$ )	142	25	6.8 ( $\pm 0.4$ )	—	—	13.34
(Eq. [4])	20.0	135 ( $\pm 1$ )	47	8.6 ( $\pm 1.1$ )	83.0 ( $\pm 2.3$ )	90	20	5.8 ( $\pm 0.3$ )	—	—	16.79
	40.0	114 ( $\pm 2$ )	55	9.1 ( $\pm 1.2$ )	85.3 ( $\pm 1.4$ )	33	17	3.0 ( $\pm 0.1$ )	—	—	2.38
DQF	0.0	—	—	6.4 ( $\pm 0.2$ )	—	120	7	11.7 ( $\pm 0.2$ )	697 ( $\pm 12$ )	0	11.60
T21	10.0	—	—	7.2 ( $\pm 0.1$ )	—	110	7	3.7 ( $\pm 0.2$ )	1714 ( $\pm 22$ )	-146	16.58
(Eq. [5])	20.0	—	—	8.0 ( $\pm 0.2$ )	—	90	9	3.2 ( $\pm 0.2$ )	1450 ( $\pm 20$ )	-108	3.20
	40.0	—	—	9.3 ( $\pm 0.1$ )	—	40	9	4.0 ( $\pm 0.2$ )	473 ( $\pm 17$ )	32	1.67
	100.0	—	—	5.1 ( $\pm 0.1$ )	—	11	7	2.8 ( $\pm 0.1$ )	300 ( $\pm 12$ )	57	0.14

<sup>a</sup> Decrease of the  $T_{31}$  peak intensity, given by A value, in the presence of LiCl, relative to the intensity before LiCl addition.

<sup>b</sup> Decrease of the  $T_{21}$  peak intensity, given by A value, in the presence of LiCl, relative to the intensity before LiCl addition (a negative value means an increased value).

studied is chemically homogeneous, with a single  $\bar{\omega}_Q$  value, rather than a powder average value. This is justified by the observation of only a small (10%) dependence of the signal lineshape on  $\tau$ , indicating that the degree of heterogeneity is small. As we are mostly interested in this work on the effects of Li<sup>+</sup> on MQF signal intensities rather than lineshapes, we did not attempt to fit these. The observed TQF signal intensity versus  $\tau$  was fitted to Eq. [4] using a single  $\bar{\omega}_Q$  value. Table 2 shows that the goodness of the fittings of the TQF data is much better if Eq. [4] is used than for Eq. [3], as shown by the parameter  $\chi^2$ , and also shows the fitted parameters obtained. The preparation time dependence of the DQF  $T_{31}$  signal intensity, obtained for the anisotropic samples ( $\bar{\omega}_Q \neq 0$ ), was also fitted by Eq. [4]. Table 2 summarizes the calculated parameters obtained from these fits, where we used the calculated  $T_{2r}$  (rise) and  $T_{2f}$  (fall) parameters, which also depend on  $\bar{\omega}_Q$ , as good approximations to  $T_{2r}$  and  $T_{2s}$  (14). The values of these parameters and their trends in the different samples are generally in good agreement with those calculated from the  $T_{31}$  component of the TQF signals (Table 2).

The modulation of the absolute value of the anisotropic  $T_{21}$  signal intensity, shown in Fig. 5, was fit by Eq. [5] (32), again with a single  $\bar{\omega}_Q$  value:

$$S(\omega, \tau) = B \exp(-\tau/T_{2f}) \sin(\bar{\omega}_Q \tau). \quad [5]$$

Table 2 also summarizes the calculated parameters obtained

from these fits. The values of the parameters  $T_{2f}$  and  $\bar{\omega}_Q$  obtained from  $T_{21}$  and  $T_{31}$  agree generally quite well.

The addition of Li<sup>+</sup> to this sample causes a small increase of  $T_{2s}$  and of  $T_{2f}$ , and a decrease of the residual quadrupolar coupling constant  $\bar{\omega}_Q$ , reflecting the replacement of Na<sup>+</sup> ions by Li<sup>+</sup> at the membrane isotropic and anisotropic binding sites. The  $T_{2f}$  values obtained from the TQF  $T_{31}$  signal show a decrease at high (>40 mM) Li<sup>+</sup> concentration, possibly reflecting ionic strength effects on the conformation of the cytoskeleton.

Figure 3B compares the intensities of the  $T_{31}$  components of TQF and DQF and the  $T_{21}$  components of DQF as a function of the Li<sup>+</sup>/Na<sup>+</sup> ratio  $\rho$ . Removal of the cytoskeleton significantly reduces the  $T_{31}$  signal intensity at all ionic strengths but has no significant effect on its percentage quenching. However, in the intact RBC membrane, addition of Li<sup>+</sup> up to 10–20 mM significantly increases the intensity of  $T_{21}$ , and only at 40 mM or higher Li<sup>+</sup> efficiently quenches this anisotropic signal.

The linewidths at half-height of the TQF and DQF signals were found to decrease by about 10% with an increase of the preparation time, which indicates the presence at the RBC membrane of nonequivalent Na<sup>+</sup> binding sites in slow chemical exchange (12). The presence of some heterogeneity of membrane binding sites is illustrated by the TQF signal linewidth for the RBC membranes in the presence of 50 mM NaCl, which decreases initially very steeply at low preparation times and stabilizes for  $\tau \geq \tau_{\max}$ . The presence of increasing Li<sup>+</sup>

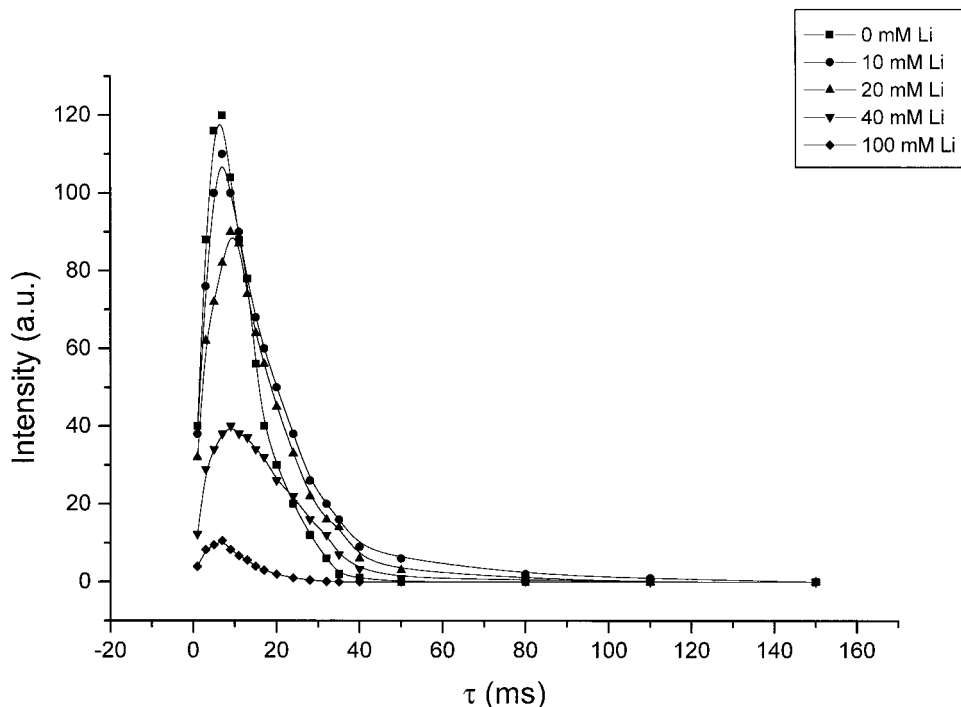


**FIG. 5.** Plot of the preparation time dependence of the intensity of the  $T_{21}$  component of the  $^{23}\text{Na}$  DQF NMR signal at increasing LiCl concentrations for unsealed RBC membranes in the presence of 50 mM NaCl at 25°C. The solid lines correspond to calculated curves using the parameters in Table 2, resulting from nonlinear least-squares fitting of the data.

concentrations causes the limiting linewidth value at high preparation time to decrease substantially in intact membranes (from 28 Hz in the absence of  $\text{Li}^+$  to 22 Hz in the presence of 100 mM  $\text{Li}^+$ ). This indicates competition of  $\text{Li}^+$  with  $\text{Na}^+$  for all types of membrane binding sites.

To help understand the involvement of the cytoskeleton in  $\text{Li}^+$  binding and  $\text{Li}^+/\text{Na}^+$  competition,  $^7\text{Li}$   $T_1$  measurements were also conducted with samples of unsealed RBC membranes and csdRBC membranes. Two types of experiments were performed: membrane samples containing 4.0 mM LiCl were titrated with 0 to 10 mM NaCl (data not shown), and alternatively, membrane samples were titrated with 2 to 14 mM LiCl in the presence of 0, 2, 5, and 8 mM NaCl (Table 3). The monoexponential approximation for the  $^7\text{Li}$   $T_1$  values of these samples is justified because their LiCl concentrations are lower than 20 mM. In fact, the  $T_1$  and  $T_2$  values of the intracellular  $^7\text{Li}$  resonance of frog hearts perfused with  $\text{Li}^+$ -containing buffer have been found to be monoexponential (47), whereas both relaxation parameters are weakly biexponential (e.g.,  $T_{1s}/T_{1f}$  is only 1.2) for 20 mM LiCl in the presence of unsealed RBC membrane (5). Also, no anisotropic membrane binding sites are present for  $\text{Na}^+$  ions, and presumably also for  $\text{Li}^+$  ions, at a total ionic strength lower than 22 mM, as shown by the present  $^{23}\text{Na}$  DQF experiments.

In the experiments where membrane samples containing 4.0 mM LiCl were titrated with 0 to 10 mM NaCl, the average protein concentration of the unsealed and the csdRBC mem-

brane samples was unchanged ( $5.50 \pm 0.02$  mg/mL and  $5.75 \pm 0.02$  mg/mL, respectively). The total phospholipid content was also comparable in all samples ( $60.6 \pm 3.0$  mg [PL]/100 mg [TP]). In the absence of  $\text{Na}^+$  (data not shown), the average ( $n = 4$ )  $^7\text{Li}$   $T_1$  values for unsealed membranes ( $7.80 \pm 0.80$  s) were not significantly different from those for the csdRBC membranes ( $8.31 \pm 0.38$  s). As the NaCl concentration increased to 10 mM, the  $^7\text{Li}$   $T_1$  values increased to  $9.92 \pm 0.50$  s

**TABLE 3**

**Calculated  $\text{Li}^+$  and  $\text{Na}^+$  Binding Constants to Unsealed and csdRBC Membranes Obtained from James–Noggle Plots of  $^7\text{Li}$   $T_1$  Data for Membrane Samples Titrated with LiCl in the Presence of Increasing NaCl Concentrations**

[NaCl] (mM)	Unsealed RBC membrane $K_{\text{Li}}^{\text{app}}$ ( $\text{M}^{-1}$ )	CsdRBC membrane $K_{\text{Li}}^{\text{app}}$ ( $\text{M}^{-1}$ )
0	$185 \pm 27$ (n=5)	$328 \pm 39$ (n=5)
2	$149 \pm 12$ (n=3)	$251 \pm 29$ (n=3)
5	$85 \pm 13$ (n=3)	$122 \pm 48$ (n=3)
8	$62 \pm 14$ (n=3)	$114 \pm 3$ (n= 3)
	$K_{\text{Na}} = 292 \text{ M}^{-1}$	$K_{\text{Na}} = 262 \text{ M}^{-1}$
	$K_{\text{Li}} = 209 \text{ M}^{-1}$	$K_{\text{Li}} = 321 \text{ M}^{-1}$
	$R^2 = 0.98^a$	$R^2 = 0.92^a$

<sup>a</sup>  $R^2$  values are correlation factors for the linear least-squares fit of  $K_{\text{Li}}^{\text{app}}$  values, obtained from James–Noggle plots of  $^7\text{Li}$   $T_1$  data, as a function of  $[\text{Na}^+]$ , according to Eq. [6].

(unsealed RBC membranes) and to  $11.25 \pm 0.21$  s (csdRBC membranes). Thus, the  ${}^7\text{Li}$   $T_1$  values increase upon  $\text{Na}^+$  addition, approaching the limiting values measured in the presence of a large excess (500 mM) of NaCl, where most of the  $\text{Li}^+$  is free ( $19.10 \pm 1.79$  s for unsealed RBC membranes vs  $15.12 \pm 0.20$  s for csdRBC membranes). This is indicative of  $\text{Li}^+/\text{Na}^+$  competition for the same isotropic membrane binding sites.

These qualitative experiments were complemented with the quantitative determination of the ion binding constants,  $K_{\text{Li}}$  and  $K_{\text{Na}}$ , to the unsealed and csdRBC RBC membranes. The membrane samples were titrated with 2 to 14 mM LiCl in the presence of 0 to 8 mM NaCl. For each titration, a  $\text{Li}^+$  binding constant was calculated using a James–Noggle plot. In the absence of  $\text{Na}^+$ , this yields a true  $\text{Li}^+$  binding constant,  $K_{\text{Li}}$ , but in the presence of increasing  $\text{Na}^+$  concentrations,  $[\text{Na}^+]_t$ , apparent  $\text{Li}^+$  binding constants are obtained, which are given by

$$K_{\text{Li}}^{\text{app}} = K_{\text{Li}}[(1 + [\text{Na}^+]_t)/K_{\text{Na}}]. \quad [6]$$

A linear least-squares fit of the  $K_{\text{Li}}^{\text{app}}$  values as a function of  $[\text{Na}^+]_t$  gave the calculated binding constants of Table 3. It can be seen that cytoskeleton depletion did not cause a statistically significant ( $p < 0.40$ ) decrease of the  $\text{Na}^+$  binding constant to the membrane. It induced a significantly ( $p < 0.029$ ) larger increase of the  $\text{Li}^+$  binding constant, from  $209 \text{ M}^{-1}$  for the unsealed RBC membrane to  $321 \text{ M}^{-1}$  for the csdRBC membrane. Thus, cytoskeleton depletion favors  $\text{Li}^+$  relative to  $\text{Na}^+$  binding, and  $\text{Li}^+/\text{Na}^+$  competition for its isotropic sites. In the absence of the cytoskeleton, direct alkali cation binding to the phosphodiester groups of the membrane phospholipids follows the relative order of  $K_b$  values ( $\text{Li}^+ > \text{Na}^+ > \text{K}^+$ ) expected for strong chelating ligands, such as phosphate or other anions of weak acids. This is illustrated by the  $K_b$  values reported for phosphate ( $K_b = 0.95$  ( $\text{Li}^+$ );  $0.75$  ( $\text{Na}^+$ );  $0.60$  ( $\text{K}^+$ )) (47). In the intact RBC membrane, the relative order of  $K_b$  values is reversed ( $\text{Li}^+ < \text{Na}^+$ ), possibly because the cytoskeleton network has a larger steric hindrance effect to binding of the  $\text{Li}^+$  ion to the membrane phosphate groups than for the  $\text{Na}^+$  ion, due to the larger hydrated radius of  $\text{Li}^+$ .

## DISCUSSION

${}^{23}\text{Na}$  MQF NMR experiments, conducted using unsealed and csdRBC membranes at two ionic strengths (5 and 50 mM NaCl) in the presence of increasing amounts of LiCl, can probe the effect of the presence and the conformation of the membrane cytoskeleton on the interaction of  $\text{Na}^+$  with the membrane binding sites and on the competition of  $\text{Li}^+$  for those sites. The observed TQF signal provided evidence for  $\text{Li}^+/\text{Na}^+$  competition for all membrane binding sites, through the odd rank  $T_{31}$  tensor, which results from evolution of the three-quantum state  $T_{33}$ . In fact,  $T_{31}$  results from both isotropic and anisotropic  $\text{Na}^+$  interactions. However, the observed DQF

results from the evolution of even and odd rank two quantum states,  $T_{22}$  and  $T_{32}$ , yielding the  $T_{31}$  and  $T_{21}$  tensors. As  $T_{21}$  only appears for anisotropic interactions, the DQF, besides providing the same information as the TQF on all types (isotropic and anisotropic) of  $\text{Na}^+$  sites and  $\text{Li}^+/\text{Na}^+$  competition through  $T_{31}$ , specifically can probe the anisotropic sites through  $T_{21}$ . Thus, the DQF  $T_{21}/T_{31}$  ratio may reflect the percentage of anisotropic sites present in a sample.

The DQF spectra of unsealed RBC membranes containing 50 mM NaCl exhibited two superimposed signals of opposite signs at lower preparation times (Fig. 4A), while at higher values the broad negative signal disappeared. This kind of signals was first observed for  ${}^{23}\text{Na}$  DQF NMR in bovine nasal cartilage (31) and later in mammalian erythrocytes (13). The appearance of the negative signal is due to the formation of the second rank tensor  $T_{21}$ , which arises when the quadrupolar interaction between the nuclei and the surroundings is not averaged to zero (31). The formation of  $T_{21}$ , with the broad negative DQF signal component, provides a good method to detect anisotropic motion of bound ions in biological systems. Removal of the cytoskeleton of the unsealed membrane at 50 mM NaCl concentration caused  $T_{21}$  to vanish and the DQF spectra exhibited a sharp positive resonance resulting from the odd ranked tensor  $T_{31}$ . In human RBCs, anisotropic motion of the intracellular  $\text{Na}^+$  was found to be due to interaction with the plasma membrane modulated by the conformation of its cytoskeleton network (12, 14, 37, 38). Variation of the medium ionic strength dramatically influences the anisotropic motion of membrane-bound cations by affecting the cytoskeletal spectrin dimer/tetramer equilibrium (14, 49). Spectrin tetramers and dimers have structures based on the left-handed three  $\alpha$ -helix bundle motif (50). At low salt levels, dissociation of the spectrin tetramers into dimers leads to a decrease in the percentage of its  $\alpha$ -helical structure (51) and loss of anisotropy of the loosened cytoskeleton network (12). In the unsealed membranes, this effect is followed by partial dissociation of the cytoskeleton from the membrane surface, as the absence of the cations prevents the shielding of the electrostatic repulsion between the negatively charged surfaces of the membrane and cytoskeleton (52). The  $T_{21}$  component of the DQF signal disappears at low (<40 mM) ionic strength (Table 1).

The preparation time dependence of the  ${}^{23}\text{Na}$  TQF and DQF NMR signal intensity for the unsealed and csdRBC membranes at 5 and 50 mM NaCl (see illustrations in Figs. 1 and 4) were analyzed and the corresponding parameters are shown in Tables 1 and 2. The TQF spectra gave only the  $T_{31}$  signal, whose maximum intensity was affected by ionic strength and the presence of the cytoskeleton network (12). An increase in the NaCl concentration in the suspending medium from 5 to 50 mM resulted in a decrease of the maximum TQF/SQ signal intensity ratio by a factor of 2.6 for the unsealed membranes, and 3.8 for the csdRBC membranes. Cytoskeleton depletion of the membranes was accompanied by a significant decrease of that TQF/SQ signal ratio (by 1.4 at 5 mM  $\text{Na}^+$ , by 3.5 at 50

mM Na<sup>+</sup>). Thus the absence of the cytoskeleton weakens the binding of Na<sup>+</sup> to the membrane sites probed by the TQF signal.

The decrease in TQF signal intensity upon LiCl addition was due to the displacement of Na<sup>+</sup> by Li<sup>+</sup> from all the Na<sup>+</sup> binding sites (isotropic and anisotropic) of the membrane. The extent of competition between these two ions depends on the ionic strength, the affinity of the lithium ion to the membrane, and the presence and integrity of the cytoskeleton. This is illustrated by the plots of Fig. 3, representing the dependence of the intensity *A* of the *T*<sub>31</sub> component of the TQF signal on the Li<sup>+</sup>/Na<sup>+</sup> concentration ratio  $\rho$ , as well as by the parameter  $\Delta A$  in Tables 1 and 2. At the same Li<sup>+</sup>/Na<sup>+</sup> ratio, the extent of competition of Li<sup>+</sup> is higher at 50 mM NaCl than at 5 mM NaCl. This could be due to the saturation of the membrane binding sites by Na<sup>+</sup> ions at this high concentration, as Li<sup>+</sup> addition causes immediate displacement of Na<sup>+</sup> since no vacant sites are available for Li<sup>+</sup> to bind. However, the percentage of quenching of the *T*<sub>31</sub> TQF signal is comparable in intact and csdRBC membranes, showing that the effect of the cytoskeleton on Li<sup>+</sup>/Na<sup>+</sup> competition for the TQF-probed sites could be detected by this technique.

This study was complemented by <sup>23</sup>Na DQF measurements on the unsealed RBC membranes at 50 mM NaCl, which simultaneously probed all sites and selectively the anisotropic membrane sites via the intensity of the *T*<sub>31</sub> and *T*<sub>21</sub> signals, respectively. Figures 3B, 4, and 5, as well as Table 2, show that when Li<sup>+</sup> is added to this sample up to a Li<sup>+</sup>/Na<sup>+</sup> ratio of 2.0, both the anisotropic *T*<sub>21</sub> signal and the *T*<sub>31</sub> signal are quenched. However, the ratio of the maximum *T*<sub>21</sub>/*T*<sub>31</sub> intensities increases from 0.6 in the absence of LiCl (*T*<sub>31</sub> predominates) to 1.2 in the presence of 40 mM LiCl (*T*<sub>21</sub> predominates) (Table 2). The predominance of *T*<sub>21</sub> vs *T*<sub>31</sub> as LiCl is added is even better illustrated by the *B/A* ratio (Table 2), which increases from 2.7 (0 mM LiCl) to 10.7 (20 mM LiCl) and then decreases to 4.2 (40 mM LiCl). This indicates that Li<sup>+</sup> competes with Na<sup>+</sup> preferentially at the isotropic membrane sites, and only at higher concentrations Li<sup>+</sup> competes for the anisotropic sites. Possibly, the former sites are of lower affinity and the latter of higher affinity for cations. Also, the increased ionic strength initially increases the number of membrane anisotropic sites. Thus, it is important to take into account the contribution of the second rank tensor *T*<sub>21</sub> in any study of DQF signal intensity (53), which has not been done in a previous study of the effect of Li<sup>+</sup> on the <sup>23</sup>Na DQF signal of RBCs (37).

There is a strong indication of the presence of nonequivalent Na<sup>+</sup> binding sites in slow chemical exchange at the membrane of intact RBCs (12). This binding site heterogeneity is much smaller in the presently studied isolated membranes, as reflected by a small dependence of the TQF and DQF signal linewidths on the preparation time. Increasing amounts of Li<sup>+</sup> causes the limiting linewidth value at high preparation time to decrease substantially in intact membranes, indicating Li<sup>+</sup>/Na<sup>+</sup> competition for all the membrane binding sites.

Previous studies, using <sup>7</sup>Li relaxation measurements in agar gels as models for the Li<sup>+</sup> molecular interactions (6), led to the suggestion that the large <sup>7</sup>Li *T*<sub>2</sub>/*T*<sub>1</sub> ratio in Li<sup>+</sup>-loaded human RBCs was due to electric field gradients on this quadrupolar nucleus when Li<sup>+</sup> transverses the SA network. Thus, it was proposed that SA could provide a major binding site for Li<sup>+</sup> in the RBCs. A later study (5) proved that it is the RBC membrane, in particular the inner leaflet with a greater percentage of anionic phospholipids, which provides the major binding site for Li<sup>+</sup>. The observed increase of the <sup>7</sup>Li *T*<sub>1</sub> values with increasing Na<sup>+</sup> concentrations to both unsealed and csdRBC membrane preparations indicates the occurrence of Li<sup>+</sup>/Na<sup>+</sup> competition for the isotropic membrane binding sites. A comparison of the calculated Li<sup>+</sup> apparent affinity constants for the unsealed and csdRBC membranes in the presence of 0 to 8 mM Na<sup>+</sup> allowed the determination of the true Li<sup>+</sup> and Na<sup>+</sup> affinity constants (Table 3). These show that the removal of the cytoskeleton increases the Li<sup>+</sup> affinity for the RBC membrane. This could be because, once the cytoskeleton is removed, the absence of the mesh-like structure of the SA network allows easier diffusion of the hydrated Li<sup>+</sup> ion toward the inner leaflet surface and enhanced binding to the more exposed anionic phospholipids. The observed small decrease of the Na<sup>+</sup> affinity for the RBC membrane upon cytoskeleton removal should reflect the less pronounced steric hindrance effect of the SA network to binding of the Na<sup>+</sup> ion, with a smaller hydrated radius, to the membrane. <sup>7</sup>Li *T*<sub>1</sub> values proved to be a technique more sensitive to quantitative Li<sup>+</sup>/Na<sup>+</sup> competition than <sup>23</sup>Na MQF, as this technique could not detect any effect of the cytoskeleton on Li<sup>+</sup>/Na<sup>+</sup> competition for the membrane isotropic sites.

Our results from <sup>23</sup>Na MQF and <sup>7</sup>Li *T*<sub>1</sub> NMR experiments with the unsealed and the csdRBC membranes demonstrate that the cytoskeleton plays only an indirect role toward Na<sup>+</sup> and Li<sup>+</sup> binding to the RBC membrane. This membrane binding could occur both to phospholipids and membrane-bound proteins, such as Band 3 protein. The SA network only discriminates between these two ions through their different hydrated radii, facilitating the diffusion of the smaller hydrated Na<sup>+</sup> ion. However, the presence of the cytoskeleton is responsible for the anisotropic motion of the bound Na<sup>+</sup> ions at the surface of the unsealed RBC membrane phospholipids and membrane-bound proteins, leading to the presence of isotropic and anisotropic sites. The conformation of the cytoskeleton network affects the extent of Na<sup>+</sup> binding to the anisotropic, higher affinity sites and the extent of Li<sup>+</sup> competition for the isotropic and anisotropic Na<sup>+</sup> sites. It will be interesting to see if a similar experimental strategy using <sup>7</sup>Li MQF methods could be developed to probe directly the molecular details of Li<sup>+</sup>/Na<sup>+</sup> competition for the RBC membrane binding sites.

